FPRINT-95-10

# A matter model for dark halos of galaxies and quasars

Franz E. Schunck*

*Institute for Theoretical Physics, University of Cologne, D-50923 Köln, Germany*

(February 2, 1995)

FERMILAB
MAR 7 1995
LIBRARY

## Abstract

We analyze the stationary spherically symmetric Einstein-massless-scalar-field equations and show numerically that the solutions, especially the scalar field, are globally regular up to the lapse function which is singular at infinity. Nevertheless, several curvature invariants are globally regular and vanish asymptotically. The asymptotic space has a deficit solid angle. The rotation curve and the density let suppose a matter model for dark halos of galaxies. High values of the redshift speak in favor of a quasar model.

PACS no.: 04.25.Dm, 95.35.+d, 98.80.-k

NAME | I.D No. | M.S.
Due 1/23/96
RETURN TO FERMILAB LIBRARY

Typeset using REVTEX

*Electronic address: fs@thp.uni-koeln.de

**Introduction.** Spherically symmetric astrophysical objects are described by the Einstein equation. The only possible vacuum solution is the Schwarzschild one, interpreted as black hole, possessing a singularity at the center and an horizon at $r = 2M$. Self-gravitating (ideal) fluids prevent such irregularities as known in the cases of white dwarfs and neutron stars [1]. Self-gravitationally bound states using photons, i.e., the Maxwell field, so-called *geons*, were found by Wheeler [2]. For constructing the spherically symmetric solutions it was necessary to have a combination of several frequencies of electromagnetic waves.

By taking scalar matter both singular and regular solutions can occur. Scalar matter, as represented by a scalar field, describes the ground state of all scalar particles which can possess mass, self-interaction, and stationarity. The stationarity is related to the conservation of particles and prevents irregularities (if one chooses the right central conditions). The so-called *boson stars* are the best example, which consist of stationary massive scalar particles [3–6]. If one adds an additionally repulsive self-interaction for each bosonic particle, the boson star can reach the size of a neutron star [7,8]. Real massive scalar particles cannot prevent singularities [9]; the same is valid for real massless scalar particles [10]. It was shown that the singularities at the center correspond to a pointlike singular event horizon whereas static, bare black holes (no naked singularities) can be endowed with no exterior scalar field [11]. Time dependent real scalar fields with regular boundaries can save the regularity, as in the case of the *oscillating soliton stars* [12]. In our Letter we show that massless stationary scalar particles produces a *globally regular* scalar field solution. Only one frequency is necessary in contrast to the *geons*.

**Einstein-scalar-field equations.** The Lagrange density of a massless self-gravitating scalar field reads

$$\mathcal{L} = \frac{1}{2}\sqrt{|\, g \,|}\Big[\frac{1}{\kappa}R + g^{\mu\nu}(\partial_\mu\Phi^*)(\partial_\nu\Phi)\Big] \,, \tag{1}$$

where $R$ is the curvature scalar, $\kappa = 8\pi G$, $G$ the gravitation constant ($\hbar = c = 1$), $g$ the determinant of the metric $g_{\mu\nu}$, and $\Phi$ the massless *complex* scalar field. Then we find the coupled system $R_{\mu\nu} - \frac{1}{2}g_{\mu\nu}R = -\kappa T_{\mu\nu}(\Phi)$ , $\Box\Phi = 0$ , where $T_{\mu\nu} = (\partial_\mu\Phi^*)(\partial_\nu\Phi) -$

$g_{\mu\nu}\Big(g^{\sigma\kappa}(\partial_\sigma\Phi^*)(\partial_\kappa\Phi)\Big)/2$ is the energy-momentum tensor and $\Box = \partial_\mu\Big(\sqrt{|\,g\,|}g^{\mu\nu}\partial_\nu\Big)/\sqrt{|\,g\,|}$ the generally covariant d'Alembertian.

For spherically symmetric solutions we use the following static line element $ds^2 = e^{\nu(r)}dt^2 - e^{\lambda(r)}dr^2 - r^2(d\vartheta^2 + \sin^2\vartheta\, d\phi^2)$, and for the scalar field the ansatz $\Phi(r,t) = P(r)e^{-i\omega t}$, where $\omega$ is the frequency.

The non-vanishing components of the energy-momentum tensor are $T_0{}^0 = \rho = -T_1{}^1 = p_r = [\omega^2 P^2(r)e^{-\nu} + P'^2(r)e^{-\lambda}]/2$ , $T_2{}^2 = T_3{}^3 = -p_\perp = -[\omega^2 P^2(r)e^{-\nu} - P'^2(r)e^{-\lambda}]/2$ , where $' = d/dr$. As equation of state, we find $\rho = p_r = p_\perp + P'^2(r)e^{-\lambda}$ .

The decisive non-vanishing components of the Einstein equation are

$$\nu' + \lambda' = \kappa(\rho + p_r)re^{\lambda} \,, \tag{2}$$

$$\lambda' = \kappa\rho r e^{\lambda} - \frac{1}{r}(e^{\lambda} - 1) \,, \tag{3}$$

and two further identically components which are fulfilled because of the Bianchi identities.

The differential equation for the scalar field is

$$P''(r) + \left(\frac{1}{2}(\nu' - \lambda') + \frac{2}{r}\right) P'(r) + e^{\lambda-\nu}\omega^2 P(r) = 0 \,. \tag{4}$$

A typical behavior of the solutions is demonstrated in Figs. 1-3; for the rest of our paper, we employ the redefined quantities $x := \omega r$ and $\sigma := \sqrt{\kappa/2}\, P$. For the numerical calculation we used a Runge-Kutta-routine of the Fortran-library IMSL. In order to get regular solutions at the origin for the system of differential equations (2), (3), and (4), we have to put the following *initial conditions*: $\sigma'(0) = 0$ and $\lambda(0) = 0$.

An important feature of this solution class is that the initial value $\nu(0)$ scales only the solution for a fixed $\sigma(0)$, i.e., an independent solution is parametrized by the square root of the central density, $\sigma(0)$. For example, take the solution for $\sigma(0) = 0.3$ together with $\nu(0) = -1$ or $\nu(0) = 1$, respectively, the minima and maxima of the scalar field or the saddle points of the density (see below), respectively, are only different by a factor $\sim 2.71$ and, hence, the whole solution.

At $\sigma(0) \simeq 0.375$, saddle points appear within the metric function $e^{\lambda}$, and for smaller initial values of $\sigma(0)$, one recognizes an oscillating behavior as for the scalar field; cf. Fig. 4.

**Regularity.** We calculate here the quadratic curvature invariant $R^2_{inv} = R^{\lambda\sigma\mu\nu}R_{\lambda\sigma\mu\nu}$ . In the case of the Schwarzschild-metric, it is $R^2_{inv} \sim 1/r^6$, i.e., it exists no singularity at the horizont $r = 2M$, but a physically important one at $r = 0$. The numerical calculation of the invariant of our model shows its global regularity [13]. The same was found for the two invariants $R_{\mu\nu}R^{\mu\nu}$ of the Ricci tensor and $R^2$ of the curvature scalar. The invariants of the irreducible decomposition of Riemann's curvature tensor show also no singularity [13]. Hence our solutions possess no relevant singularity.

**Asymptotic solution.** From the numerical results and Eq. (4), we guess the following asymptotic differential equation of the scalar field (4) $\sigma'' + \frac{2}{x}\sigma' + \sigma \simeq 0$ ($' = d/dx$) which has the solution

$$\sigma(x) \simeq A\frac{\sin(x)}{x} + B\frac{\cos(x)}{x} , \tag{5}$$

where $A, B$ are some constants. This asymptotic solution, together with ansatz $\Phi(r,t) = P(r)e^{-i\omega t}$, describes *asymptotically* a spherical wave. Thus, our solution is a superposition of massless scalar particles moving in- and outward the center.

The scalar field just as the energy density $\rho$ and the pressures $p_r$ and $p_\perp$ vanish asymptotically. There, the energy density reads (for $B = 0$; cf. Fig. 5 with a *Mathematica* plot of)

$$\rho(x) \simeq A^2\left[\frac{1}{x^2} - \frac{\sin(2x)}{x^3} + \frac{\sin^2(x)}{x^4}\right] . \tag{6}$$

For $B \neq 0$ the same correspondence between asymptotic formula and numerical results can be found, only the formula (6) is more complicated.

The general solution of Eq. (3) is $e^{-\lambda} = 1 - M(x)/x$ with the mass function $M(x) = \int_0^x \rho(\zeta)\zeta^2 d\zeta$ . Asymptotically, we find (cf. Fig. 6)

$$M(x) \simeq A^2\left[x + \frac{\cos(2x) - 1}{2x}\right] . \tag{7}$$

A linearly radial increase of the mass function exhibits also the gravitational field of a global monopole or global texture, cf. [14,15]. But in our case, the mass function does not only diverge linearly but it also oscillates around the linear increase. The result is an infinite mass which corresponds to a boson star with an infinite number of nodes.

Because the numerator and the denominator of the quotient $M(x)/x$ diverges for $x \to \infty$, we can use de l'Hospital's rule. At infinity, the metric potential approaches the value $e^{-\lambda} \to C^2 := 1 - A^2$, where $C^2 < 1$. After a redefinition of the coordinate $x \to C^{-1}x$ , the space has a deficit solid angle. The area of a sphere of radius $x$ is not $4\pi x^2$, but $4\pi C^2 x^2$; cf., e.g., analogous results for global monopoles and global textures [14,15].

Following equation (2), the second metric potential behaves asymptotically like $e^{\nu} \to x^K$, where $K = 2A^2/C^2 = 2(1/C^2 - 1) > 0$. By looking into the curvature invariants, we recognize that only $\nu'$, $\nu''$, and (no-inverse) powers of them appear; they vanish asymptotically.

**Energy density and tangential pressure.** A further investigation of the solutions shows that the energy density $\rho$ or the radial pressure $p_r$, respectively, decrease terracedly (Fig. 5). A similar behavior shows the energy density of a rotating neutron star (cf. [16]). We find also the relation $\mid \rho \mid \geq \mid p_\perp \mid$, where the tangential pressure $p_\perp$ as the scalar field oscillates sinusoidally around zero. From the equation of state, one recognizes that at each extremum of the scalar field $\sigma$ the difference between radial and tangential pressure vanishes. Then, the equation of state $\rho = p$ of a *stiff* fluid arises (Fig. 5).

**Scaling of the solutions.** As we have seen from the redefined quantities, $\omega$ scales the physical dimension of the solution. Table I shows for different values of $\omega$ the density and the mass at different radii. For very high energies $\omega$ of the scalar field our stars possess a high density and their mass is low at small distances of the center. But for very low energies $\omega$ the density is very low and the mass approaches values of galaxies or galaxy clusters within scales much smaller than the ranges of galaxies or galaxy clusters. It is remarkably that all values of central densities are possible, among them values for molecule clouds, white dwarfs, neutron stars, and extremely beyond them.

**Rotation curves.** A spherically symmetric mass distribution $M(x)$ gives in Newtonian

theory the gravitational acceleration (left side) $M(x)/(2x^2) = v^2(x)/x$, where $v(x)$ (in units of $c$) is the circular rotation velocity within the centrifugal force (cf. Fig.7). This equation determines the so-called *rotation curve.* This approximation is valid for small initial values $\sigma(0)$. The velocity depends also only on the initial value $\sigma(0)$ as the density, for example. By investigating the radial dependence of the rotation curve for large $\sigma(0)$, first a maximum at a maximal value $v_{max} \simeq 0.521\,c$ is reached going over into a minimum and thereafter we find a limit value near $0.5\,c$. These values can be interesting for accretion disks or quasars.

The rotation curves for galaxies or galaxy clusters should show a decrease $v \simeq \sqrt{1/r}$ at the point where the visible matter ends. Instead one observes flat rotation curves within and beyond the galaxies [with the help of neutral hydrogen (HI) which surrounds galaxies] [17]. A linear increase of the mass function of galaxies and galaxy clusters can be derived from these observations [18]. Several models are discussed where either the Newtonian gravity [19] or new non-interacting matter (dark matter) [20] are introduced to solve this problem. For several classes of gravitational theories, it was recently shown that the introduction of dark matter is necessary [21]. For the dark matter one expects a $1/x^2$ behavior of its density. But this is just what our model provides.

For the initial value $\sigma(0) = 0.0007$ we find a limit value of about 150 km/s for the rotation velocity as it is reached by HI in the galaxy NGC3198 [22]. Our model provides for the inner sphere with radius 130 pc a mass of about 100 $M_\odot$. This is too few in order to explain the observed central masses in galaxies which are associated with black holes [23]. For our Galaxy, newest results [24] let expect a mass of $10^6$ $M_\odot$ within 0.1 pc.

**Gravitational Redshift — Quasars.** The gravitational redshift $z$ of a static spherically symmetric mass distribution is determined by $z = e^{(\nu(A_1)-\nu(A_0))/2} - 1$, where $A_0$ corresponds to the emitter and $A_1$ to the receiver, both in rest. Typical redshifts for quasars are about $z \sim 2$ which needs $e^{(\nu(A_1)-\nu(A_0))} \sim 9$. It is a well-known fact that the redshift-distance-relation is only valid up to $z \sim 0.46$ [25]. Furthermore, Arp had found some 'bridges' between bright galaxies and quasars where both objects have very different redshift values [25]. From our model it is no problem to find such large redshift values; take, for example, the solution

in Fig. 3 with $e^{\nu(1)} = 3.406$ and $e^{\nu(7.72)} = 30.654$, the nine times higher value. It provides also a natural explanation for the 'bridges'; while the Doppler effect is responsible for the redshift of the bright galaxy, the neighbor, the quasar, has an enormous redshift produced by the mass (where we have omitted the influence of the Doppler effect).

**Discussion.** We have presented a solution class where one can find both Newtonian and general relativistic objects. The Newtonian creation could be responsible for the dark matter which is missing in galaxies and galaxy clusters expressed by their flat rotation curves. The general relativistic objects provide large gravitational redshifts because of their mass. They could be a model for quasars. The high rotation velocities possible for these objects could be an explanation for the large energy contributions seen in quasars. Both objects have in common the behavior of the energy density and the tangential pressure, the form of the rotation curve and the with the distance linearly increasing mass.

## ACKNOWLEDGMENTS

We would like to thank Peter Baekler, Ralf Hecht, Friedrich W. Hehl, Eckehard W. Mielke, and Yuri N. Obukhov for helpful discussions and comments. Support was provided by the Deutsche Forschungsgemeinschaft, project He 528/14 – 1.

## REFERENCES


[1] S. L. Shapiro and S. A. Teukolsky: *Black Holes, White Dwarfs and Neutron Stars*, (J. Wiley, New York 1983).

[2] J. A. Wheeler, *Phys. Rev.* **97**, 511 (1955).

[3] D. J. Kaup, *Phys. Rev.* **172**, 1331 (1968).

[4] T. D. Lee and Y. Pang, *Phys. Rep.* **221**, 251 (1992).

[5] Ph. Jetzer, *Phys. Rep.* **220**, 163 (1992).

[6] F. V. Kusmartsev, E. W. Mielke, and F. E. Schunck, *Phys. Rev.* D **43**, 3895 (1991).

[7] E. W. Mielke and R. Scherzer, *Phys. Rev.* D **24**, 2111 (1981).

[8] M. Colpi, S. L. Shapiro, and I. Wasserman, *Phys. Rev. Lett.* **57**, 2485 (1986).

[9] M. Fabbrichesi and R. Iengo, *Phys. Lett.* B **292**, 262 (1992); Ph. Jetzer and D. Scialom, *Phys. Lett.* A **169**, 12 (1992).

[10] P. Baekler, E. W. Mielke, R. Hecht, and F. W. Hehl, *Nucl. Phys.* B **288**, 800 (1987).

[11] A. I. Janis, E. T. Newman, and J. Winicour, *Phys. Rev. Lett.* **20**, 878 (1968); J. D. Bekenstein, *Phys. Rev.* D **5**, 1239 (1972) and ibid. **5**, 2403 (1972).

[12] E. Seidel and W.-M. Suen, *Phys. Rev. Lett.* **66**, 1659 (1991).

[13] F. E. Schunck: *Selbstgravitierende bosonische Materie*, Ph. D. thesis, Cologne (1994).

[14] M. Barriola and A. Vilenkin, *Phys. Rev. Lett.* **63**, 341 (1989).

[15] N. Turok and D. Spergel, *Phys. Rev. Lett.* **64**, 2736 (1990).

[16] J. L. Friedmann, J. R. Ipser, and L. Parker, *Astrophys. J.* **304**, 115 (1986).

[17] P. J. E. Peebles: *Principles of Physical Cosmology* (Princeton, Princeton University Press, 1993); E. W. Kolb and M. S. Turner: *The Early Universe* (Redwood City, Addison

Wesley Publ., 1990); D. W. Sciama: *Modern cosmology and the dark matter problem* (Cambridge, Cambridge University Press, 1993).

[18] J. P. Ostriker, P. J. E. Peebles, and A. Yahil, *Astrophys. J.* **193**, L1 (1974).

[19] J. Bekenstein and M. Milgrom, *Astrophys. J.* **286**, 7 (1984).

[20] V. Trimble, *Ann. Rev. Astron. Astrophys.* **187**, 425 (1987).

[21] V. V. Zhytnikov and J. M. Nester, *Phys. Rev. Lett.* **73**, 2950 (1994).

[22] T. S. van Albada, J. N. Bahcall, K. Begeman, and R. Sanscisi, *Astrophys. J.* **295**, 305 (1985).

[23] J. Travis, *Science* **264**, 1405 (1994); G. P. Collins, *Physics Today* **47**, No. 8, 17 (1994).

[24] R. Genzel, D. Hollenbach, and Ch. H. Townes, *Rep. Prog. Phys.* **57**, 417 (1994).

[25] S. Mitton (ed.): *Cambridge Enzyklopädie der Astronomie* (Orbis-Verlag für Publistik, München, 1989).

## TABLES

TABLE I. Order-of-magnitude estimation for non-self-interacting massless scalar matter. We put the frequency $1/\omega = 1$ cm, $10^9$ cm (radius of earth), $10^{11}$ cm (radius of sun), $10^{15}$ cm (radius of our solar system), $10^{18}$ cm = 1 Ly. Further: $\omega$ in units of eV; the density $\rho$ at the center and at a distance of $x = 200$; the mass at a distance of $x = 10$. The values of the density and the mass are taken for the solution in Figs. 5 and 6.

| $\omega$ [1/cm] | $\omega$ [eV] | $\rho(0)$ [g/cm$^3$] | $\rho(200)$ [g/cm$^3$] | $M(10)$ [g] |
|---|---|---|---|---|
| 1 | $10^{-5}$ | $10^{27}$ | $10^{21}$ | $10^{28}$ |
| $10^{-9}$ | $10^{-14}$ | $10^{9}$ | $10^{3}$ | $10^{37}$ |
| $10^{-11}$ | $10^{-16}$ | $10^{5}$ | $10^{-1}$ | $10^{39}$ |
| $10^{-15}$ | $10^{-20}$ | $10^{-3}$ | $10^{-9}$ | $10^{43}$ |
| $10^{-18}$ | $10^{-23}$ | $10^{-9}$ | $10^{-15}$ | $10^{46}$ |

## FIGURES

FIG. 1. The stationary massless scalar field $\sigma = \sqrt{\kappa/2}\,P$ depending on the dimensionless coordinate $x = \omega r$ under the initial values $\sigma(0) = 1$ and $\nu(0) = 1$. Figures 2-6 are generated for the same initial values. The frequency $\omega$ scales here the radial coordinate $r$ whereas, in the case of the boson star, the mass of the scalar field takes on this role [6].

FIG. 2. The gravitational potential $e^{\lambda(x)}$.

FIG. 3. The gravitational potential $e^{\nu(x)}$.

FIG. 4. The gravitational potential $e^{\lambda(x)}$ for the initial values $\sigma(0) = 0.2$ and $\nu(0) = 0$.

FIG. 5. The energy density $\rho$ (—) and the tangential pressure $p_\perp$ (−−) [both in units of $\omega^2/\kappa$] in the interval of $x = 200$ up to $x = 300$. One recognizes very clearly the terraced decrease of the energy density. The matter behaves like stiff matter for $d\rho/dx = 0$.

FIG. 6. Overall linear radial growth of the mass $M(x)$ $[1/(\omega\kappa)]$. The function oscillates around the linear radial increase.

FIG. 7. The rotation curve for $\sigma(0) = 0.0007$ and $\nu(0) = 0$. The curve is flat for large $x$. The limit velocity is about 150 km/s.

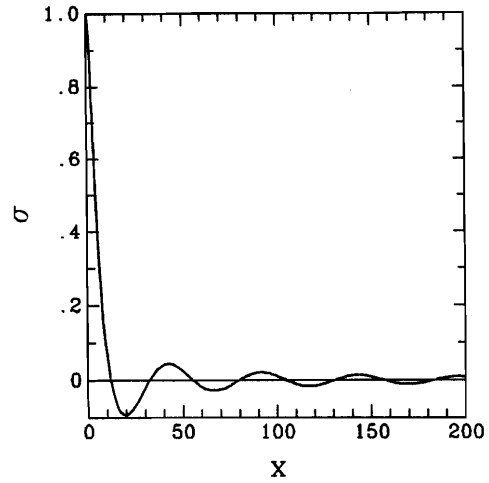


Fig. 1:

Schunck: A matter model ...; PRL

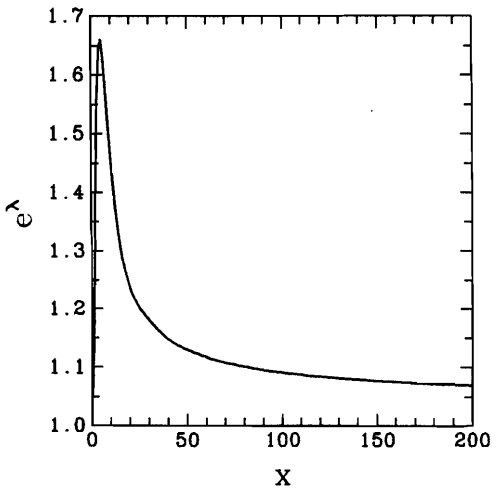


Fig. 2:

Schunck: A matter model ...; PRL

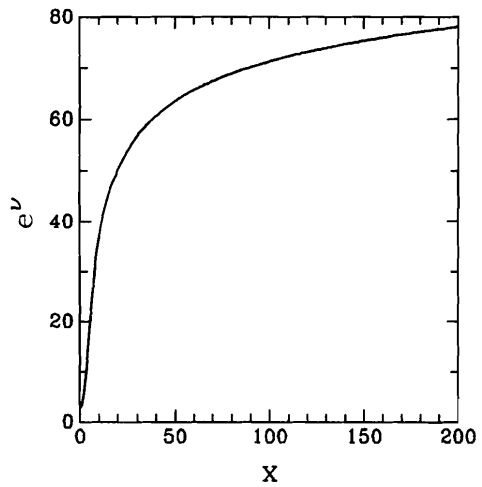


Fig. 3:

Schunck: A matter model ...; PRL

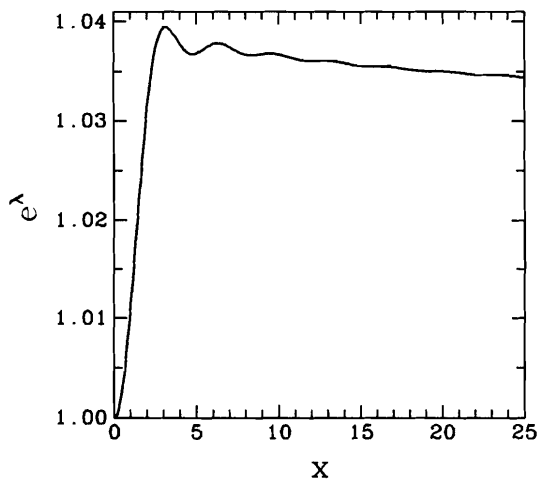


Fig. 4:

Schunck: A matter model ...; PRL

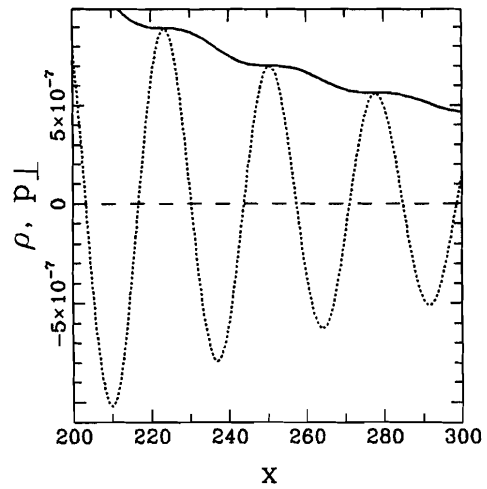


Fig. 5:

Schunck: A matter model ...; PRL

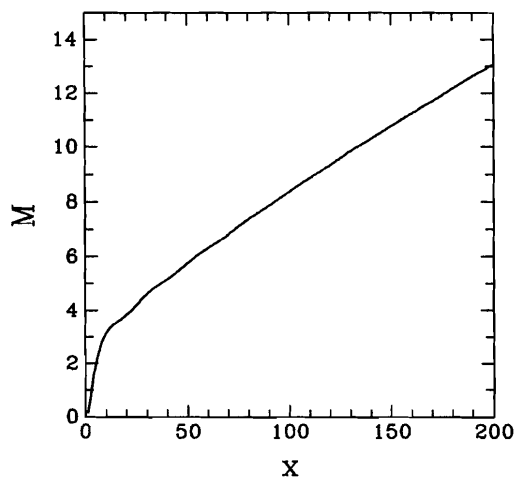


Fig. 6:

Schunck: A matter model ...;PRL

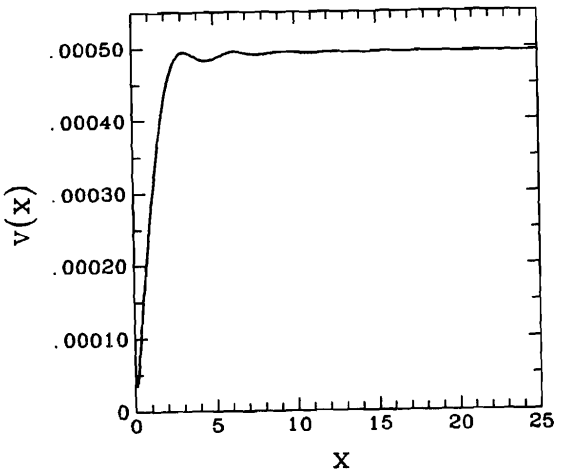


Fig. 7:

Schunck: A matter model ...; PRL